Campaign of aerodynamic measurements in a wind tunnel

Domingo, C.; Fortuny, J.; Gallegos, J.M.;
Orriols, G. and Roset, M.
Universitat Politècnica de Catalunya, UPC BarcelonaTECH
(Under the supervision of Prof. D. Crespo and Dr. J.L. Gutiérrez)

This paper introduces different ways to obtain aerodynamic results with the help of a wind tunnel. In Section I, the drag force on a cylindrical profile is measured with a scale and also computed from pressures measured at the surface of the cylinder, obtaining matching results. In Section II, lift and drag coefficients are computed for a symmetrical wing profile at different speeds and angles of attack using two different methods; the dependence of the coefficients on the angle is found to fit theoretical models. Section III is devoted to measuring the wind speed at the wake of a cylinder by means of a hot wire anemometer in order to obtain a turbulence map and an indirect measure of the drag force, which narrowly fits the results from Section I.

Keywords: wind tunnel, hot wire anemometer, winged profile, aerodynamics.

I. CYLINDER PROFILE

A. Introduction

There are different methods to study the drag force exerted by the wind on a cylinder. The following two are compared in this section:

1. Directly using the scale attached to the wind tunnel
2. Using the partial forces measured with the Pitot tube

The cylinder studied is 30 cm long and has a radius $r = 3.2$ cm.

B. Methodology

The pressure has been measured for different orientations of the hole: between 0° and 180° every 10°, 0° degrees being the orientation where the wind points to the hole. For every orientation there are 20 measures evenly distributed during 10 s.

The measures have been taken for $f_{\text{tunnel}} = 25$ Hz, which means (assuming a linear relation between the speed of the wind and the frequency) $v_{\text{wind}} = 16.66$ m/s.

To calculate the force (per unit of length) acting on the cylinder using the pressures on each angle, the following expression can be used:

$$F = \int_C P(\theta)\cos\theta \mathrm{d}l = \int_0^{2\pi} P(\theta) r\cos\theta \mathrm{d}\theta = \\ = \int_0^{360} P\left(\frac{2\pi\alpha}{360}\right)\cos\left(\frac{2\pi\alpha}{360}\right)\frac{2\pi r}{360}\mathrm{d}\alpha,$$

where r is the radius and C is the circumference of the cylinder. Since there are a discrete number of measures and even symmetry can be assumed:

$$F \approx \frac{2\pi r}{36}\left[P(0°) + 2\sum_{\alpha=1}^{17} P(10\alpha)\cos(10\alpha) - P(180°)\right]$$

Assumptions to evaluate the error:

1. α has an error of 0.5 degrees.
2. the error of the measurement of P is its standard deviation.
3. the error of α and P are independent (the error squared is the sum of the squares)

Thus:

$$\Delta F_\alpha = \sqrt{\left(\frac{\mathrm{d}F_\alpha}{\mathrm{d}P}\Delta P\right)^2 + \left(\frac{\mathrm{d}F_\alpha}{\mathrm{d}\alpha}\Delta\alpha\right)^2} = \\ = \frac{2\pi r}{36}\sqrt{(\Delta P)^2\cos^2\alpha + \left(\frac{2\pi\Delta\alpha}{360}\right)^2 P^2\sin^2\alpha}$$

C. Results

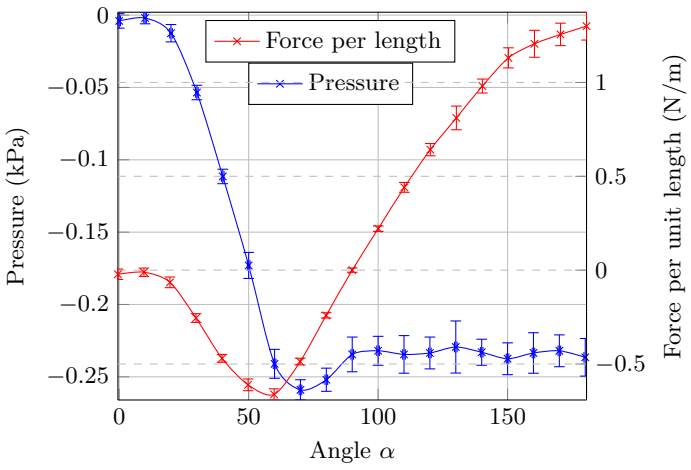

FIG. 1. Pressure and force per unit length dependence respect to α

D. Conclusions

The force obtained directly measuring with the scale was 2.611 N. The force obtained by calculating the partial forces was (2.716 ± 0.365) N. Thus, a quite accurate result is obtained. One of the possible causes for this little difference is the fact that the cylinder is finite.
It is also interesting to observe in FIG.1 that not only the partial pressure changes, but also the size of the standard deviation does.

II. WINGED PROFILE

A. Introduction

It is possible to study the lift coefficient, C_L, and drag coefficient, C_D, of a winged symmetric profile (wingspan of 0.3 m and chord of 0.15 m) for different angles of attack and different velocities of the wind. This has been done using an AFA TQ Equipment three component balance that allows the measurement of the lift force, L, and drag force, D, applied to the balance and a Pitot tube to determine the velocity of the wind.

By analyzing the pressure in different points of the wing it is also possible to estimate the drag and the lift without using the balance. This measurement will be presented for a specific speed of the wind in order to compare the results with the ones obtained with the balance and discuss the effect of having a finite wing (creation of vortexes, for example – see [1]).

B. Methodology

The measurements were done for three different velocities of the wind: 13 m/s, 27 m/s and 33 m/s that correspond to Reynolds of 2.3×10^5, 4.8×10^5 and 5.9×10^5 respectively. Therefore in all cases there were turbulent flow conditions.

For every velocity of the wind the lift and the drag were measured for angles of attack from $-9°$ until $10.5°$ making measures every $1.5°$. $0°$ mean that the wing is in horizontal position and it was possible to fix this value by looking at the angle for which there was no lift (the wing is symmetric). Positive angles correspond to a positive lift in the wing.

In every measurement C_L and C_D can be found using:

$$L = \frac{\rho {v_\infty}^2 S C_L}{2} \tag{1}$$

$$D = \frac{\rho {v_\infty}^2 S C_D}{2} \tag{2}$$

Where ρ is the density of the air. v_∞ is the velocity of the air far away from the wing and is determined using the proportional relation between the frequency of rotation of the engine and the speed of the wind. S is the surface of the wing.

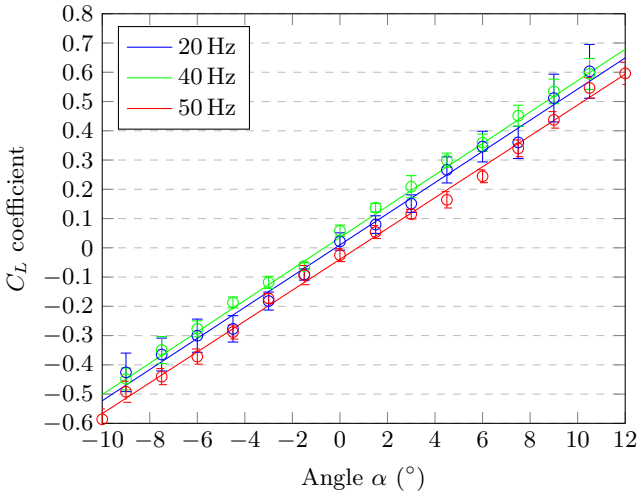

FIG. 2. C_L coefficient dependence of angle α at a wind tunnel speed corresponding to 20 Hz, 40 Hz and 50 Hz in the engine.

For the wind speed of 13 m/s C_D and C_L were also calculated using the 20 pressure sensitive probes along the chord. This was done approximating L and D in a similar fashion that we did with the cylinder. In this case it is useful to approximate the wing with an attack angle of α as two planes with inclination α (for the upper and lower surfaces). Doing this considerations:

$$D = \sum_{\text{lower surface}} P_i \Delta x_i \sin\alpha - \sum_{\text{upper surface}} P_i \Delta x_i \sin\alpha$$

$$L = \sum_{\text{lower surface}} P_i \Delta x_i \cos\alpha - \sum_{\text{upper surface}} P_i \Delta x_i \cos\alpha$$

where Δx_i have been adjusted taking into consideration the distribution of the probes along the wing. Using this expressions it is possible to obtain C_L and C_D as explained in (1) and (2).

C. Results and Discussion

FIG. 2 and 3 show the values we have obtained for the lift coefficient C_L and the drag coefficient C_D at angles ranging from $-10°$ and $10°$ approximately. Each color corresponds to one of the velocities. Errors in FIG. 2 and 3 have been computed considering a precision of 1 m/s for velocities, and the errors for velocity and forces have been assumed independent.

For a fixed angle, we observe that C_L and C_D give approximately the same value for the three speeds that we have studied. This confirms that C_L and C_D are well defined physical variables.

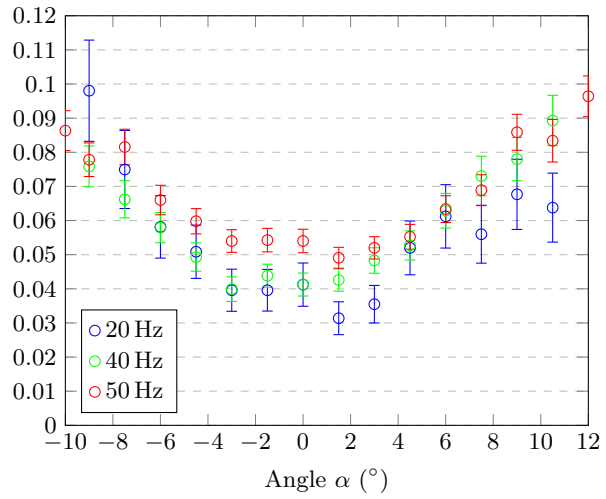

FIG. 3. C_D coefficient dependence of angle α at a wind tunnel speed corresponding to 20 Hz, 40 Hz and 50 Hz in the engine.

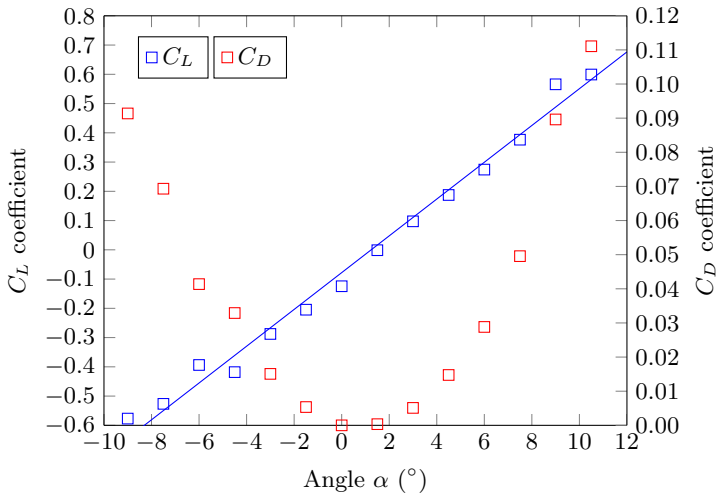

FIG. 4. C_L and C_D coefficient dependence of angle α at a wind tunnel speed corresponding to 20 Hz according to pressure measurments.

As observed in 2, C_L depends linearly with respect to α. The lines of the linear fit of the experimental points have the following equations. For 20 Hz: $y = 3.0516x + 0.0099$, for 40 Hz: $y = 3.0749x + 0.0349$ and for 50 Hz: $y = 3.0218x - 0.0394$ (in this case the equations consider that x is in radians).

Tanking into account [2] the slope of C_L respect to α for a finite wing should satisfy:

$$\frac{\mathrm{d}C_L}{\mathrm{d}\alpha} = \frac{2\pi}{1 + 2\pi/\pi AR} = \pi \tag{3}$$

Since $AR = \frac{30}{15}$ is the relation between the wingspan and the chord of the profile. Therefore the values of the slopes coincide with this theory.

The C_D curve is approximately symmetrical with respect to $\alpha = 0$. This is consistent with the fact that, disregarding the effect of gravity, the air flow must be the same setting the wing profile at angle α and at angle $-\alpha$ for all α. That is because the wing has an horizontal plane of symmetry. It can also be seen that C_D increases when $|\alpha|$ increases. This is reasonable, as a higher angle of attack means that a large surface is facing the air flow, which results in a higher drag force and higher C_D.

Using the second method, FIG. 4 presents the plot obtained for the drag coefficient and the one obtained for the lift coefficient.

Considering that x is in radians, the equation obtained for the linear plot is: $y = 3.6028x - 0.078$. In this case, the value of the slope is bigger than the slope calculated using the balance (see FIG. 2). This can be explained saying that some of the effects of a finite wing were neglected in this measurement (since the pressure probes are in the middle of the wing). For an infinite wing the slope should be 2π (from (3) and making AR to infinity) so it makes sense that the slope is between π and 2π.

D. Conclusions

As a conclusion, both methods can be used to obtain the variation of the drag and lift coefficients for small angles of attack, where the dependence is linear. It is also observed that using the pressure measurements, the start of non-linearity can be observed around 11° but no measures where done after this value.

Another observation is that the value of the slope using the pressure method is bigger than using the balance which means that the values are different for small and big angles but give us the same result around 4°-6°. We expect this result to appear due to the presences of vortexes disturbing the pressure measurements.

III. HOT WIRE ANEMOMETER

A. Introduction

As a last experiment, two hot wire anemometer probes were used with a double aim: on one hand obtaining an estimate of the turbulence of the wind in the wake of a cylinder; on the other hand, having a third measure for the drag force of the cylinder, complementing those found in Section I.

A Constant Temperature Anemometer (CTA) has been used. This device can measure the speed of the air from the voltage required to maintain the temperature of a thin metal wire constant, as it is cooled by the wind. This voltage is then translated to a speed provided a calibration process has been performed. Note that the device can only detect the modulus of the velocity, but gives no information about its direction, in contrast to the Pitot tube; in contrast, it is more precise.

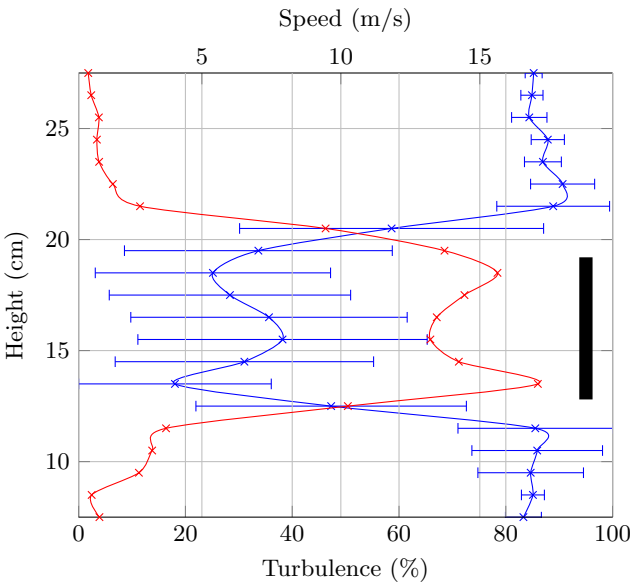

FIG. 5. The speed detected by the CTA is plotted in blue, with error bars corresponding to the standard deviation. The turbulence intensity behind the cylinder is also shown in blue as a percent. Both are represented as a function of height from the ground of the tunnel. The projection of the position of the cylinder is included in black as a reference.

B. Methodology

Two CTAs are introduced in the wind tunnel: one is kept fixed in a position that is not affected by the presence of the cylinder; the other one is placed in different vertical positions centered behind the cylinder, so that we can record wind speeds at different heights relative to the center of the cylinder. These heights are controlled by a ruler placed on top of the chamber.

The tunnel frequency of 25 Hz, as in Section I B, which corresponds to a wind speed of roughly 17 m/s. A software is used to convert the measured voltages into speeds, after providing it with calibration data. It will be set to record 1024 measurements at a frequency of 1 kHz.

In order to compute the drag force exerted on the cylinder by the wind, by the law of action-reaction it is enough to compute the rate of change of the loss of momentum of the air: $F = -\Delta\dot{p}$. Assuming a steady flow, we have

$$F = -\Delta(\dot{m}v) = \int_S \rho(v_\infty^2 - v^2)\mathrm{d}S, \qquad (4)$$

where S is a transverse section of the tunnel, v_∞ is the speed before interacting with the cylinder and v is the speed after the cylinder.

C. Results

The average speed detected by the anemometer placed far from the cylinder was 15.49 m/s with a standard deviation of 0.50 m/s. This corresponds to a turbulence of 3%.

The speed as a function of height for the second anemometer is represented in FIG. 5 together with the turbulence. Notice that the standard deviation, and hence also the turbulence intensity, of the velocities when they are close to zero is underestimated by the measurements, because all are taken as positive since the anemometer cannot detect their direction. Therefore the turbulence plotted in FIG. 5 might be smaller than the real one.

The value of the drag force computed from (4) by considering 1 cm-wide strips of area is (3.67 ± 1.04) N. The error comes essentially from quadratic propagation of the standard deviations in the speed.

D. Conclusions

The obtained value for the drag force is significantly higher than the ones found in Section I D but still compatible. This is comprehensible, since those were direct measurements of the dynamics of the cylinder, and this is an indirect measurement of the effect it produces in the wind. Possible sources of error include loss of speed in the heating of the gas and the assumption that the measured velocity is in the direction of the tunnel, which need not be the case and with a hot wind anemometer it is not possible to check.

It is also observed that the cylinder displaces the air going towards it creating a very turbulent regime (with more than 60% turbulence intensity) behind it.

IV. ACKNOWLEDGEMENTS

We would like to close this paper by thanking Dr. Crespo and Dr. Gutiérrez for their help with this project, assuring us the measurements were correct, indicating us how to analyze data properly and supporting us with all the material we needed.

We also thank the Faculty of Aerospace Engineering of Castelldefels (EETAC) for letting us do the experiments with their wind tunnel. Finally we would like to thank Dr. Pere Bruna for the learning opportunity.

[1] Milne-Thomson, L. M. *Theoretical aerodynamics*, 1966.

[2] J. D. Anderson, *Fundamentals of Aerodynamics*, McGraw-Hill, pp.380 (2001)